UDC 621.314: 621.311.6 https://doi.org/10.20998/2074-272X.2023.3.02

V.I. Milykh, V.P. Shaida, O.Yu. Yurieva

Analysis of the thermal state of the electromagnetic mill inductor with oil cooling in stationary operation modes

Introduction. *An electromagnetic mill (EMM) for the technological processing of various substances, which is based on the stator of a three-phase induction motor, is being studied. The stator winding has an increased current density, so the mill is provided with a system of forced cooling with transformer oil.* ***Problem.*** *Currently, there are no works on the thermal state calculation of the EMM with the given design and oil cooling. Therefore, the study of such EMMs thermal state is relevant, as it will contribute to increasing the reliability and efficiency of their work.* ***Goal.*** *Formation of a mathematical model of the thermal state of the electromagnetic mill inductor and the analysis of its heating in stationary modes of operation with cooling by transformer oil.* ***Methodology****. The problem of calculating the thermal state, namely the temperature distribution in the main parts of the electromagnetic mill, is solved by the equivalent thermal resistance circuit method. The design of the EMM is provided in a sufficiently complete volume, and on this basis, a corresponding equivalent thermal replacement circuit is formed, which is supplemented by an equivalent hydraulic circuit of oil passageways. An explanation is provided for the composition and solution of the equations algebraic system that describes the distribution of temperatures by the constituent elements of the EMM.* ***Results****. The thermal calculation results of the electromagnetic mill showed that the maximum heating temperature is much lower than the allowable one for the selected insulation class. According to the hydraulic scheme, the necessary oil consumption, its average speed and the corresponding pressure at the inlet of the intake pipe are determined, which are at an acceptable level. It is noted that the rather moderate temperature state of the inductor and the hydraulic parameters of the oil path are facilitated by such innovations in the design of the EMM as the loop double layer short chorded winding and axial ventilation channels in the stator core.* ***Originality****. Now EMM thermal equivalent circuits with air cooling only have been presented. Therefore, the developed thermal circuit of the oil-cooled inductor is new and makes it possible to evaluate the operating modes of the EMM.* ***Practical value.*** *The proposed technical solutions can be recommended for practical implementation in other EMMs. Taking into account the identified reserves of the EMM temperature state, a forecast was made regarding the transition from its oil cooling to air cooling. But the use of air cooling requires a change in the design of the EMM.* References 34, tables 2, figures 5.

Key words: **electromagnetic mill, forced cooling of the inductor with oil, analysis of the thermal state of the mill, method of equivalent thermal circuits, analysis of hydraulic parameters.**

Проблема*. Досліджується електромагнітний млин (ЕММ) для технологічної обробки різних речовин, який виконано на базі статора трифазного асинхронного двигуна. Обмотка статора має підвищену густину струму, тому для млина передбачена система примусового охолодження трансформаторною оливою. Наразі робіт з розрахунку теплового стану ЕММ з наданою конструкцією і охолодженням оливою не представлено. Тому дослідження теплового стану таких ЕММ є актуальним, бо сприятиме підвищенню надійності та ефективності їх роботи.* ***Метою*** *статті є формування математичної моделі теплового стану індуктора електромагнітного млина та аналіз його нагріву у стаціонарних режимах роботи з охолодженням трансформаторною оливою.* ***Задача*** *розрахунку теплового стану, а саме – розподілу температури в основних частинах індуктора електромагнітного млина, розв'язується методом еквівалентних теплових схем. Конструкція ЕММ надана у достатньо повному обсязі і на цій основі сформована відповідна еквівалентна теплова схема заміщення, яка доповнена еквівалентною гідравлічною схемою шляхів проходження оливи. Надано пояснення щодо складання та розв'язання алгебраїчної системи рівнянь, які описують розподіл температур по складовим елементам індуктора ЕММ.* ***Результати*** *теплового розрахунку індуктора ЕММ показали, що максимальна температура нагріву значно менша за допустиму для обраного класу нагрівостійкості ізоляції. За гідравлічною схемою індуктора визначено необхідні витрати оливи, її середню швидкість і відповідний тиск на вході у впускний патрубок, які знаходяться на допустимому рівні. Зазначено, що досить помірному температурному стану індуктора і гідравлічним параметрам тракту оливи сприяють такі нововведення в конструкцію ЕММ, як двошарова скорочена петльова обмотка статора і аксіальні вентиляційні канали в осерді статора. Натепер були представлені теплові еквівалентні схеми ЕММ лише з повітряним охолодженням. Тому розроблена теплова схема індуктора з охолодженням оливою є новою і дає можливість оцінки режимів роботи ЕММ.* Бібл. 34, табл. 2, рис. 5.

Ключові слова: **електромагнітний млин, примусове охолодження індуктора оливою, аналіз теплового стану млину, метод еквівалентних теплових схем, аналіз гідравлічних параметрів.**

Introduction. Devises (apparatus) with a vortex layer of ferromagnetic elements or, abbreviated, vortex layer devices (VLDs), are quite well known and are used in various industries, agriculture and communal economy [1-5].

Despite the rather significant number of VLDs manufactured by the end of the last century, their introduction into industrial production was held back by a number of reasons. Among them is the lack of a clear methodology for designing VLDs [6, 7] and the need to take into account the purpose of a specific device, which forced each device to be designed separately. A significant obstacle is the cyclical mode of operation of the equipment, which requires automation of the process of feeding and unloading the processed raw materials [3].

In the last two decades, the direction of development and implementation of VLDs received a powerful stimulus due to the relevance of global trends in the development of production. First of all, the increase in the cost of energy carriers, and the introduction of VLDs instead of traditional mills allows to reduce electricity costs [2, 6].

Secondly, the competition among global manufacturers has led to the demand to improve the quality of manufacture products and the efficiency of

existing technological processes. Here, too, VLDs came in handy [5, 8-11].

Thirdly, requirements for environmental protection in production and everyday life. The use of VLDs for the treatment of wastewater with organic or industrial pollution allows to significantly improve the quality of cleaning and reduce its cost.

At the present time, the most common are the VLDs for grinding substances, which due to their purpose have received the name of electromagnetic mills (EMMs), one of the options of which is considered in this work.

There are several large companies that manufacture VLDs for various purposes, and small enterprises that specialize in VLDs for only one purpose. An example of large enterprises is the well-known Globecore Company, Germany, one of whose branches is located in the city of Poltava, Ukraine. The most common product of this company is EMM type AVS-100 [12]. Also known is the EMM for crushing copper ore [13], created by Project SYSMEL, which has an automated loading/unloading system and a cooling system.

Depending on the purpose of EMM, there are peculiarities of the functioning of such devices, their construction and design methods. Therefore, the study of EMM, taking into account the specifics of their application, is an urgent issue.

Analysis of previous studies. The work [1], devoted to the theory of the functioning and structure of VLDs, is still considered basic for their design [4, 5].

Currently, there are several dozen scientific teams in different countries of the world conducting EMM research, the fields of which are different. In fact, most of these scientific groups go through the same stages of EMM research, starting with its design, manufacturing a sample, and ending with the improvement of its parameters. In this sense, a group of Polish scientists engaged in EMM research for crushing copper ore is quite indicative [10]. In their publications [3, 6, 13-15] over the last decade, they presented the results of EMM research, starting from the development of the mill design, the loading/unloading system, the raw material processing quality control system, and the installation control system.

The main part of the EMM is an inductor powered by a three-phase AC network and creates a rotating magnetic field [4, 7]. Under the action of this magnetic field, ferromagnetic elements located in the working chamber perform chaotic motion [1, 2, 7]. The inductor together with the working chamber and grinders (ferromagnetic) elements are active parts that ensure the processing. The structure of these parts directly affects the efficiency of the EMM [3, 7], therefore, the largest number of works is devoted to the study of their influence.

Currently, EMM manufacturers use two variants of the design of the inductor: the first variant, traditional, with clearly marked poles [3]; the second one – with ambiguous poles based on the stator of an induction motor [16].

Despite the different constructions of the inductor, most of them are made bipolar ($2p = 2$) with a rotation frequency of the magnetic field of 3000 rpm. From the very beginning [1] and further, it is believed that a homogeneous magnetic field in the working chamber is optimal for ensuring the uniformity of movement of mill elements. This is facilitated by the sinusoidal distribution of the magnetomotive force (MMF) by the boring of the stator core. This is quite close provided by a non-equal-pole structure with a three-phase winding, as in induction motors, which is adopted in a number of developments. An example of such a development is shown in [17], where a theoretical-experimental study of an inductor – a borrowed stator of a conventional induction motor – was performed.

The work [1] provides an analytical method for determining the dimensions and parameters of the EMM inductor, but it does not provide the necessary accuracy of calculations due to the accepted simplifications [6, 7]. In [4, 7], the problem of sufficiently accurate determination of the magnetic field and electromagnetic parameters of the EMM inductor is solved by their calculations by numerical methods using modern software complexes.

In [4], the numerical field analysis of the EMM inductor was performed using the FEMM software. Calculation interdependencies of electromagnetic quantities and the corresponding characteristics of the EMM inductor were obtained. But this is done on the assumption that the ferromagnetic elements are placed in the working chamber uniformly, as it was forced to do in [1].

In fact, the grinding elements in the working chamber move chaotically, because they constantly collide with each other and the inner surface of the working chamber. The development of a mathematical model of the trajectory of movement of grinding elements in the working chamber of the EMM was carried out in [7, 18], where it was established that the complex nature of the dependence of the electromagnetic force acting on the grinding elements on various factors precludes the possibility of obtaining an analytical solution.

A significant part of the works [4, 6-8] is devoted to determining the number and optimal size ratio of grinding elements, as well as the filling factor of the working chamber. The study of the influence of the dimensions of the working chamber on the efficiency of grinding of raw materials was carried out in [6].

Another area of EMM research is the assessment of the influence of the inductor operating mode and its control [4, 6, 7, 19] and the raw material processing time on the quality parameters of its processing [9, 14, 20, 21]. Studies of the efficiency of EMM were carried out in [7, 9, 10].

To ensure an effective grinding process, the EMM inductor must create a magnetic field with fairly high parameters in the working chamber. For example, in [9] it is indicated that the average value of magnetic flux density in the working chamber of the EMM prototype is 0.153 T, and in [4] the value of 0.2 T is considered. To ensure such parameters of the magnetic field in the working chamber, the inductor winding must have a high value of current density. Accordingly, for heat removal, it is necessary to create effective cooling of the inductor [6, 7].

In practice, three types of cooling are used: air, oil and water.

In EMM for grinding copper ore [3, 9], the inductor is cooled by air using fans. The work [16] also investigates EMM with traditional air cooling inherent in the stator of an induction motor.

But the most widespread is oil cooling, it is used in their EMMs by both the Globecore Company and a significant number of small manufacturers [4, 7, 10].

The issues of inductor cooling have received somewhat less attention compared to other studies, which is explained by the cyclical nature of the operation of a significant number of EMMs. That is, thanks to the short-term mode of its work, it had time to cool down.

The study of the thermal state of the EMM, created on the basis of the stator of an induction motor with air cooling, was carried out in [16, 22].

In [22], the results of calculating the temperature distribution, obtained by the method of equivalent thermal circuits, were compared with experimental data obtained earlier by EMM thermography [23].

But in general, unfortunately, works related to the study of the thermal state of oil-cooled EMMs are currently not presented. This may be due both to the increase in the complexity of thermal calculations, compared to air-cooled EMMs, and to significant time costs. Also, there is no clear criterion for choosing a cooling method for EMM, which would allow the designer to be clearly defined during its development.

Unlike EMM, the methods of thermal analysis of electric machines are well developed, and the choice of cooling system is structured [24]. Also, water cooling systems of electric machines for cars, based on the type of water «shirt» [25], are being researched and used quite intensively.

Therefore, it can be considered that the task of researching the thermal state of the EMM with forced oil cooling is relevant, as it will allow to increase the reliability and efficiency of the EMM.

For such research, there is already a promising improved design of EMM based on the stator of a three-phase induction motor, which was formed in the process of development evolution and provided in works [19, 26].

The goal of the article is the formation of a mathematical model of the thermal state of the inductor of an electromagnetic mill and the analysis of its heating in stationary modes of operation with cooling by transformer oil.

Object of study. The electromagnetic system of the improved EMM presented in [19, 26] is shown here in Fig. 1. The inductor is powered by a three-phase network with phase voltage of 100 V and frequency of 50 Hz.

The initial design parameter is the magnetic flux density of 0.12 T in the center of the empty working chamber. This state of the EMM is considered an ideal non-working course. In other modes, which are given in [19] and discussed later in the article, the chamber contains ferromagnetic elements, and the coefficient of its filling with them was considered to be equal to 0.1.

The electromagnetic calculation of the inductor is performed by analogy with the methods given in [4, 19, 26].

For reasons of the technological process, the radius of the inner surface of the chamber r_{ki} = 0.047 m and the axial length of the stator core l_a = 0.25 m are set. By calculation, the radii of core boring r_{si} = 0.06 m and its outer surface r_{se} = 0.109 m are determined.

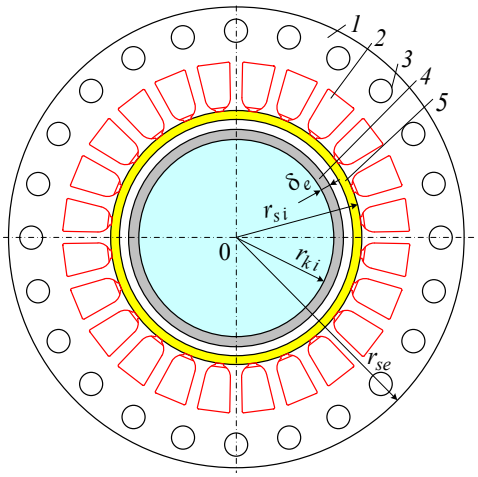

Fig. 1. Electromagnetic system of the rotating magnetic field inductor: *1* – laminated stator core; *2* – three-phase winding; *3* – ventilation channels; *4* – shell of the working chamber with thickness of δ_e =5 mm; *5* – insulating pipe

The insulating pipe *5* (Fig. 1) is made of plastic, and through the air gap of 4 mm from it there is a shell of the working chamber *4* made of stainless steel. This tube holds and insulates the inductor winding in the slots and prevents oil from entering the gap. Also the pipe together with the air gap distance the working chamber from the zone of the teeth of the stator core with an nonuniform distribution of the magnetic field, which contributes to the uniform distribution of ferromagnetic elements in the chamber.

In a thermal sense, the insulating pipe and the air gap practically exclude heat transfer between the oil and the working chamber, so this path is not taken into account in the thermal calculation of the inductor.

To improve the operational properties of the inductor, two steps that have not yet been tested have been taken. Instead of the usual concentric diametral winding of the stator, a shortened loop winding is introduced, which allows to eliminate the asymmetry of the phase windings and to ensure an increase in the homogeneity of the magnetic field in the working chamber of the inductor – this is shown in [26]. In addition, axial ventilation channels are provided in the core of the stator, which is aimed at improving the cooling of the electromagnetic system of the inductor. At the same time, this is facilitated by a more «sparce» structure of the thinner frontal parts of the stator loop winding, which increases their cooling surface.

So, this is how the task of assessing the thermal state of the EMM inductor and the ability to ensure its acceptable level by cooling with transformer oil arose.

For a complete understanding of the operation of the EMM and an explanation of its electromagnetic component, Fig. 2 shows the structure of the inductor according to [19, 26], which actually ensures the operation of the mill, although this is not the main topic of the article. Here the instantaneous distribution of currents in the three-phase winding, the corresponding direction of action of its MMF F_s and the picture of the

2D magnetic field in the operating mode with the presence of ferromagnetic elements are shown.

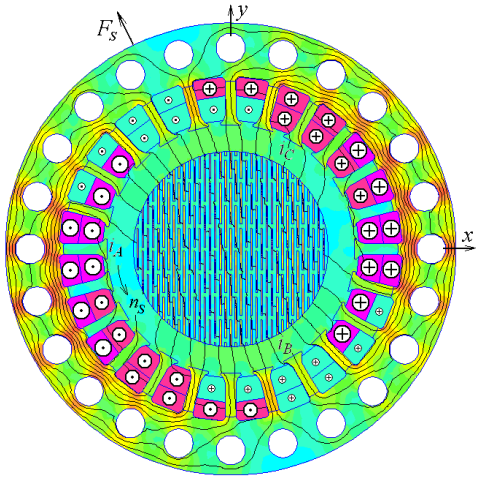

Fig. 2. Magnetic field in the cross section of the inductor at rated load

The well-known FEMM software based on the Finite Element Method was used to calculate the magnetic field, as indicated in [4, 19].

The magnetic field is rotating, and ferromagnetic elements move with it, ensuring the necessary processing of the substance in the working chamber.

It is known [4, 19, 26] that for electromagnetic calculations of the inductor, its electromagnetic system is enough, which is given in Fig. 2.

However, to calculate the thermal state of the inductor, it is necessary to take into account its entire 3D structure. The structure of the EMM along with the main dimensions is shown in Fig. 3 in its longitudinal section. Together with the cross section in Fig. 1, it provides a fairly complete picture of the entire structure of the inductor.

Research methods and results. The thermal calculation of the EMM inductor with forced cooling by the flow of transformer oil must take into account the heating of the oil along the length of the inductor. Therefore, it is desirable to use 3D modelling of the temperature field, for example, using the Finite Element Method. It is known that for this the calculation model is divided into separate elements in the form of tetrahedra. With the complex structure and rather large dimensions of the design of the EMM inductor, especially the frontal parts of its winding, the number of model elements must be very large. The experience of calculating even a 2D axisymmetric model of an electric machine [27] shows that the duration of the calculation will be excessive, as will the necessary computer resources.

In this case, the only possible solution for solving the formulated problem is the application of the method of equivalent thermal circuits (ETC).

Thermal calculation of electric machines using the ETC method ensures the reliability of the results with an error of up to 5-10 % [28, 29]. It allows to take into account the temperature change in the thin layer of insulation and to obtain the temperature distribution along the length of the inductor and in the entire volume of the EMM. This method was used to calculate the thermal state of a similar EMM, but with differences in design and at air cooling [22].

The necessary reference data for thermal calculation were obtained from modern reference books [30, 31]. Such data are the thermal conductivity λ of copper, electrical steel grade 2212, air, transformer oil, materials of the frame and end shields – steel St35, the inner tube of the stator – fiberglass, slot insulation of heat resistance class B; specific heat capacity c and mass density ρ; kinematic viscosities v of air and transformer oil; dynamic viscosity μ of the latter.

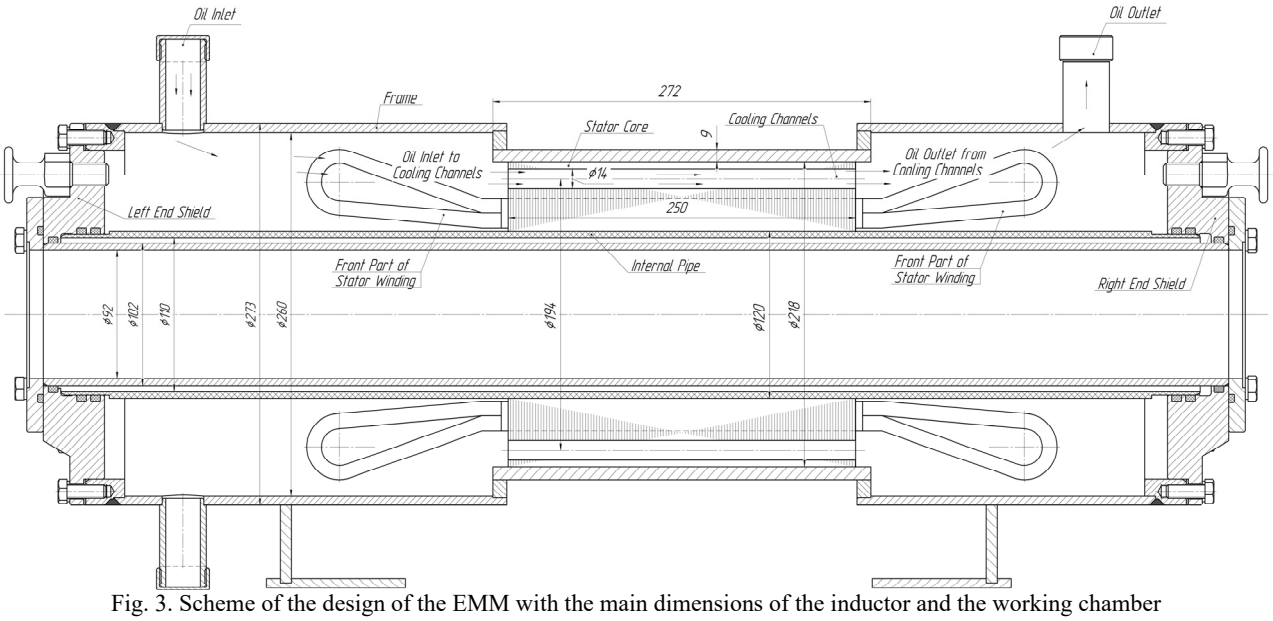

Fig. 3. Scheme of the design of the EMM with the main dimensions of the inductor and the working chamber

The thermal calculation of the inductor was performed for the temperature of the transformer oil at its inlet θ_{oil} = 20 °C, the ambient temperature θ_{ens} = 20 °C.

The movement of the heat flow for the proposed design of the inductor (Fig. 1, 3) is directed from the slot part of the winding to its frontal parts and to the teeth and

back of the inductor core. This heat from the core with the addition of magnetic losses in it is transferred to the frame, and from the ends of the core to the cooling transformer oil. Part of the heat from the core is transferred to the inner insulating pipe (Fig. 1), which is made of plastic. But heat is practically not transferred through it and the air gap, so the effect of heat from the grinding elements in the working chamber is not taken into account.

From the front parts of the winding, heat is transferred to the cooling oil, which enters from the inlet port, passes through the left front part of the winding, the cooling channels inside the inductor core, through the right front part of the winding and exits through the outlet port. The heat from the transformer oil is transferred to the end shields, parts of the frame and the insulating pipe, free from the core. Due to the fact that the transformer oil is heated when passing through the inductor, the thermal system is asymmetrical. That is, the side of the inductor at the inlet of the transformer oil is colder than the side at the outlet.

On the basis of the scheme of the movement of the heat flow, the ETC of the EMM inductor is built (Fig. 4).

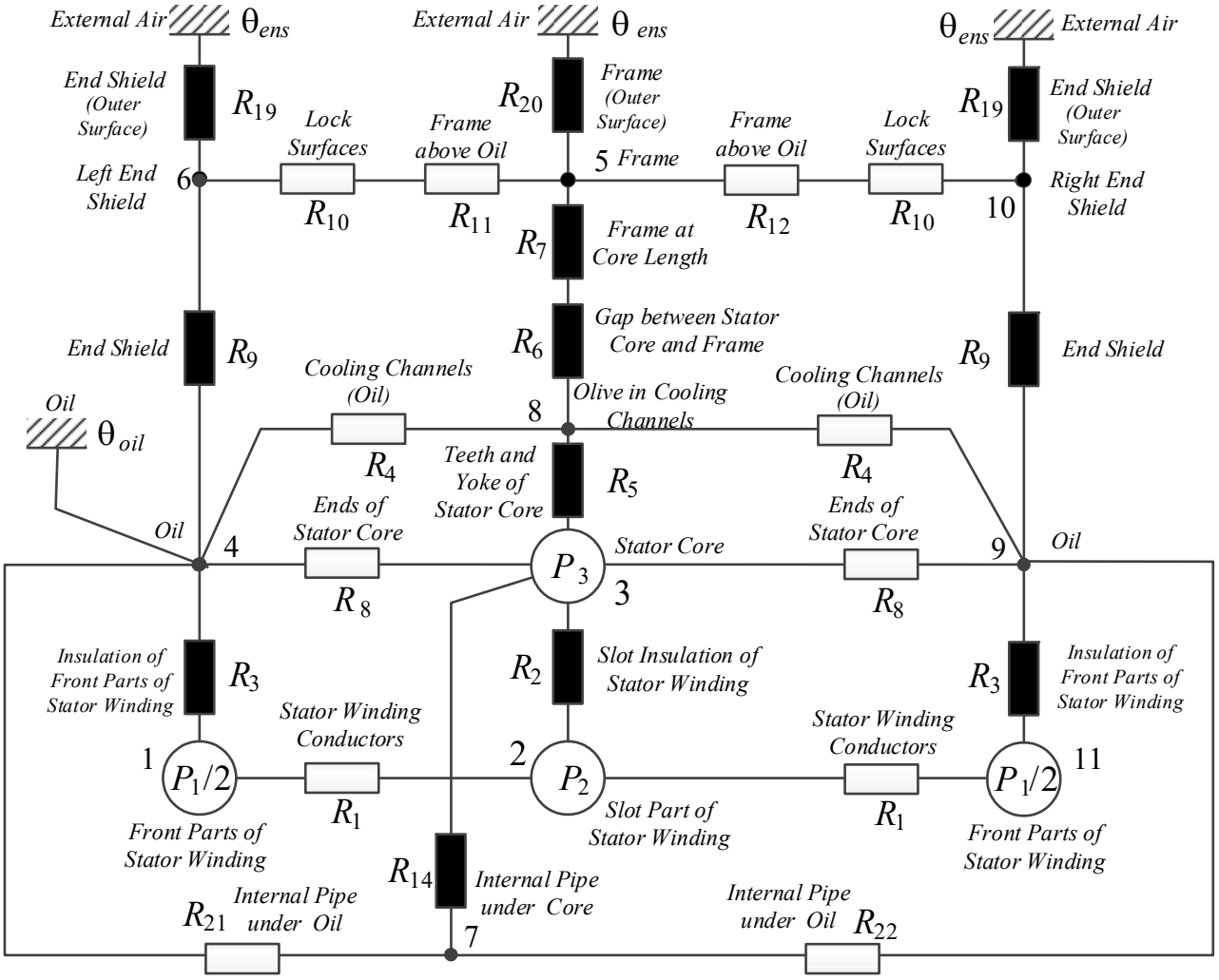

Fig. 4. Equivalent thermal circuit of the EMM inductor

In the inductor, separate homogeneous parts are distinguished, which in ETS are nodes 1–11: slot and two front parts of the winding, stator core, transformer oil in the space of the front parts and in the cooling channels of the inductor core, frame, end shields, internal insulating pipe. The sources of heat in the EMM inductor are its winding and core. Electric and magnetic losses in them were determined based on the results of electromagnetic calculation, as described in [4, 19].

Electrical losses are divided between the slot and front parts of the winding in proportion to the lengths of these parts and determine the power of the heat sources P_1 and P_2. The power of the heat source of node 3 (teeth and back of the stator core) P_3 is determined by magnetic and additional losses. The rest of the nodes do not have their own heat sources, so their power is zero. The principles of determining these losses are given in [4, 19, 26].

The equivalent thermal scheme has two reference nodes – nodes with defined temperature. These are the ambient air node with temperature θ_{ens} and the inlet transformer oil node with temperature θ_{oil}.

Thermal resistances of structural elements are determined according to generally accepted formulas, which depend on the structural element and its cooling

conditions [29]. The calculated expression for the thermal resistance is determined by the nature of the heat exchange.

Conductive thermal resistances were determined using reference thermal conductivities λ according to the general formula [29]:

$$R_\lambda = \frac{\delta}{\lambda \cdot S}, \quad (1)$$

where δ is the thickness of the thermal wall of the EMM structural element; S is the surface area of the wall.

Convective thermal resistances were determined through heat transfer coefficients α. Their values were chosen based on the experience of thermal calculations of structurally similar electric machines. The general formula for calculating convective thermal resistance [29]:

$$R_\alpha = \frac{1}{\alpha \cdot S}, \quad (2)$$

where S is the heat transfer surface area.

For example, the heat transfers from the surfaces of the end shields and the inductor frame were determined from [23] and were 124 W/(m^2·°C) and 87 W/(m^2·°C). The rest of the heat transfers were determined based on the experience of thermal calculations of induction motors [32, 33].

Thermal connections between nodes of the equivalent thermal circuit are determined by thermal resistances that do not depend on temperature. The determination of these resistances between the nodes of this scheme was carried out by analogy with the rules for solving the problems of calculating electric circuits.

For a simpler solution of the system of equations characterizing the thermal state of each node, thermal conductivities were used. The mutual thermal conductivities between the nodes are inverse values of the thermal resistances of the branches of the equivalent thermal circuit. The intrinsic thermal conductivities of the nodes are the sum of the conductivities of the branches entering the node. Thermal conductivities between nodes where there is no direct connection are zero.

In order to systematize the designations, the indices next to the letters correspond to the numbers of the circuit nodes.

Determination of the temperatures of equivalent nodes of the thermal circuit occurs with the help of the system of algebraic equations, which consists of heat balance equations of heat sources.

The system of equations in matrix symbols has the form:

$$\boldsymbol{\Lambda} \times \boldsymbol{\theta} + \boldsymbol{P} = 0, \quad (3)$$

where $\boldsymbol{\Lambda}$ is the thermal conductivity matrix; $\boldsymbol{\theta}$ is the node temperature matrix; $\boldsymbol{P}$ is the power of heat sources matrix.

The equations are compiled for all nodes of the equivalent thermal scheme, except for reference nodes. For the nodes of the equivalent thermal circuit that have a thermal connection with the reference nodes, the combined losses are added to the power of the node – the product of the temperature of the reference node θ_{oil} or θ_{ens} and the thermal conductivity between the node and the reference point Λ_{4oil}, Λ_{5ens}, Λ_{6ens} or Λ_{10ens}:

$$\boldsymbol{P} = \begin{bmatrix} P_1 \\ P_2 \\ P_3 \\ P_4 + \theta_{oil} \cdot \Lambda_{4oil} \\ P_5 + \theta_{ens} \cdot \Lambda_{5ens} \\ P_6 + \theta_{ens} \cdot \Lambda_{6ens} \\ P_7 \\ P_8 \\ P_9 \\ P_{10} + \theta_{ens} \cdot \Lambda_{10ens} \\ P_{11} \end{bmatrix}. \quad (4)$$

The solution of the system of equations is the temperature values of the elements of the inductor design – nodes of the equivalent thermal circuit (see Fig. 4): the frontal part on the side of the transformer oil inlet (node 1); slot part (node 2); stator core (node 3); transformer oil at the inlet (node 4); frame (node 5); end shield on the side of the transformer oil inlet (node 6); internal pipe (node 7); oil in the cooling channels (node 8); of transformer oil at the outlet (node 9); end shield on the side of the transformer oil outlet (node 10); front part of the winding on the side of the outlet of the transformer oil (node 11).

To perform the thermal calculation, the open access software SMath Studio [34] was developed. The calculation was performed for four stationary modes of operation of the inductor: ideal non-working course (INW); «working» non-working course (WNW), when the ferromagnetic elements are loaded, and there is no processed raw material; nominal load mode (NLM), when there are both elements and raw materials; maximum load mode (MLM) [19]. The values of stator winding current I_s, input power P_{in}, output power P_{out}, electrical losses P_{els}, magnetic losses P_{mags}, required for thermal calculation, are summarized in Table 1.

Table 1

The value of the quantities required for thermal calculation

Mode	I_s, A	P_{in}, W	P_{out}, W	P_{els}, W	P_{mags}, W
INW	66,5	4142	–	4101	41
WNW	35,0	1190	0	1139	51
NLM	36,0	3074	1827	1206	47
MLM	46,0	5727	3715	1969	43

The results of the calculations are given in Table 2. Exceeding the temperature of the oil at the outlet above the temperature of the oil at the inlet in the modes is: INW – 22 °C, WNW – 6 °C, NLM – 7 °C, MLM – 11 °C.

As predicted in [19], the INW mode is the most stressful both from the point of view of the current load and the heating of the elements of the inductor structures. Therefore, it is very undesirable to have the inductor in this mode for a long time, that is, without ferromagnetic elements in the working chamber.

In other modes, and primarily in the nominal load mode, the temperature state of the inductor is quite moderate. The following factors contributed to this:

1) the reasonable selection of the stator winding voltage relative to the given level of magnetic flux density in the working chamber;

2) the use of a two-layer shortened stator loop winding with thinned and sparce frontal parts, which also ensures the symmetry of the three-phase inductor system and improved distribution of the magnetic field in the stator core and the working chamber;

3) the use of axial ventilation channels in the stator core.

Table 2

Comparison of thermal calculation results for four oil-cooled inductor operating modes

Mode	Node numbers of the circuit and their temperature, °C					
	1	2	3	4	5	6
INW	62	71	44	31	30	30
WNW	32	34	27	23	23	23
NLM	32	35	27	23	23	23
MLM	40	45	31	26	25	25
	Node numbers of the circuit and their temperature, °C					
	7	8	9	10	11	
INW	41	36	53	46	77	
WNW	26	25	29	27	36	
NLM	26	25	30	28	37	
MLM	30	28	36	32	47	

Note that if we take the temperature of the environment and transformer oil at the level of 40 °C, as is done for electric machines, then all the temperatures in Table 2 increase accordingly. The highest temperature of the frontal part then reaches almost 100 °C, and this already requires serious attention.

To complement the thermal calculation, hydraulic calculation is performed in parallel with it, of course, here too. The corresponding equivalent hydraulic circuit of the EMM inductor shown in Fig. 5 is linear and consists of serially connected sections. It contains sections with the following hydraulic resistances: inlet nozzle (path resistance Z_1), exit to the space under the frame (sudden expansion of the channel Z_2), space under the frame to the frontal parts (path resistance Z_3), entrance to the space of the frontal parts (sudden narrowing of the channel Z_4), space above the frontal parts (path resistance Z_5), entrance under the core ring (sudden narrowing of the channel Z_6), the core ring (path resistance Z_7), entrance to the cooling holes (sudden narrowing of the channel Z_8), cooling holes (path resistance Z_9), exit from the cooling holes (sudden expansion of the channel Z_{10}), core ring (path resistance Z_{11}), exit from the core ring (sudden expansion of the channel Z_{12}), space above the frontal parts (path resistance Z_{13}), entrance to the space under the frame (sudden expansion of the channel Z_{14}), space under the frame to the exhaust nozzle (path resistance Z_{15}), inlet to the exhaust nozzle (sudden narrowing of the channel Z_{16}), exhaust nozzle (path resistance Z_{17}).

In the core, 24 cooling channels are placed parallel to each other. Their hydraulic resistances Z_8, Z_9 and Z_{10} make up the parallel branches of the hydraulic circuit with the number $n_{ok} = 24$.

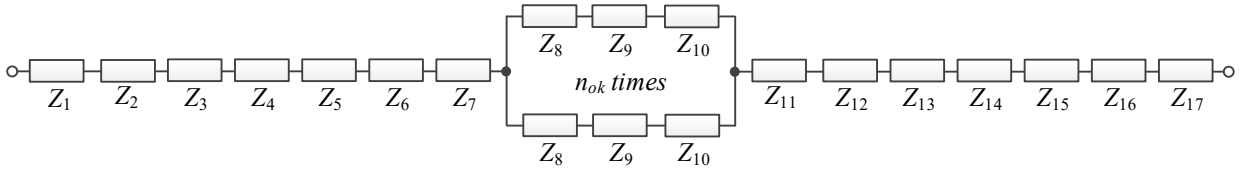

Fig. 5. Equivalent hydraulic circuit of the EMM inductor

Determination of the required oil consumption Q_v is required during the thermal calculation:

$$Q_v = \frac{k \cdot \Delta P}{C_{oil} \cdot \rho_{oil} \cdot \Delta\theta}, \quad (5)$$

where k is the coefficient that takes into account that not all heat is removed by oil, $k = 0.8$; ΔP is the total losses in the inductor (we assume the «most loaded» thermal mode), $\Delta P = 4142$ W; C_{oil} is the specific heat capacity of transformer oil; $C_{oil} = 1666$ J/(kg·K); ρ_{oil} is the mass density of transformer oil; $\rho_{oil} = 880$ kg/m^3; $\Delta\theta$ is the permissible temperature excess of the oil during its movement along the hydraulic path, $\Delta\theta = 22$ °C.

Substitute the value of $\Delta\theta$ into (5) and we have oil consumption $Q_v = 1.03\ 10^{-4}$ m^3/s.

The speed of oil movement depends on the oil consumption Q_v and the cross section of the corresponding section of the hydraulic path S_i. Let's determine the average speed of the oil at the entrance to the inlet pipe

$$V_{in} = \frac{Q_v}{S_{in\,p}}, \quad (6)$$

where $S_{in\ p}$ is the cross-sectional area of the inlet pipe, $S_{in\,p} = 491$ mm^2.

Substitute the value of $S_{in\ p}$ into (6) and we obtain the speed of oil movement $V_{in} = 0.21$m/s.

The hydraulic resistance of the i-th section of the hydraulic path is determined by the formula from [29]:

$$z_i = \xi_i \cdot \frac{\rho}{2 \cdot S_i^2}, \quad (7)$$

where ξ_i is the coefficient of hydraulic resistance of the i-th section of the hydraulic path; ρ is the mass density of the cooling medium; S_i is the cross-sectional area of the i-th section of the hydraulic tract.

After calculating the hydraulic resistances of individual sections, the total hydraulic resistance of the equivalent circuit z_Σ according to Fig. 5 is established, namely:

$$z_\Sigma = 5.46 \cdot 10^9 \text{ (N s}^2\text{)/m}^8.$$

The total pressure flow at such a hydraulic resistance is determined by the formula

$$\Delta P_{G\Sigma} = z_\Sigma \cdot Q_v^2, \quad (8)$$

and is equal to 57.9 Pa or 0.0006 atm.

Taking into account the identified reserves of the temperature state of the mill, as well as the hydraulic state of the oil path, it is possible to make a forecast regarding

the transition from oil cooling to air cooling. For this purpose, estimated thermal and hydraulic calculations were performed with air cooling according to the circuits shown in Fig. 4, 5. They showed that the use of air as a cooling medium while maintaining the structure of the EMM inductor and the close temperature level is technically very difficult, and therefore this option is impractical to implement.

As a result, by further developing the topic of switching to air cooling of the mill, it is possible to allow an increase in the temperature of its inductor elements within the permissible available reserve, as well as the use of a completely or partially open design of the inductor, that is, a significant change in the design of its frame.

Conclusions.

1. Electromagnetic mills (EMMs) find new applications both in industry and agriculture. Thanks to the introduction of research by scientists, EMMs are increasingly moving from laboratory to industrial applications. But there are still insufficiently researched issues of creation and calculation of EMM inductor oil cooling systems.

2. A mathematical model of the thermal state of the EMM inductor in stationary operating modes with its cooling by transformer oil is formed. The model contains its equivalent thermal circuit and the corresponding system of heat balance equations, and is supplemented with an equivalent hydraulic circuit of oil movement paths along with the formulas of the corresponding parameters.

3. According to the formed model, the thermal calculation of the EMM inductor was performed for four modes of its operation. The obtained temperature data of the constituent elements of the inductor show that they are at a level far enough from the critical one for the applied insulation class B, and the adopted design of the EMM inductor ensures its reliable cooling.

4. According to the estimated calculation, a forecast was made that the use of air for cooling the EMM inductor requires the use of an open structure of its body, that is, a significant change in design.

5. Further work will be devoted both to the improvement of the EMM inductor cooling system with oil, and to the design and calculation studies of its air cooling system.

Conflict of interest. The authors of the article declare that there is no conflict of interest.

REFERENCES

1. Logvinenko D.D., Sheljakov O.P. *Intensifikacija tehnologicheskih processov v apparatah s vihrevym sloem* [Intensification of technological processes in apparatus with a vortex layer]. Kiev, Tehnika Publ., 1976. 144 p. (Rus).

2. Voitovich V.A., Kart M.A., Zakharychev E.A., Tarasov S.G. Vortex-layer devices as import-substituting equipment to produce paints and adhesives. *Polymer Science, Series D*, 2017, vol. 10, no. 2, pp. 153-155. doi: https://doi.org/10.1134/S1995421217020253.

3. Wolosiewicz-Glab M., Foszcz D., Gawenda T., Ogonowski S. Design of an electromagnetic mill. Its technological and control system structures for dry milling. *E3S Web of Conferences*, 2016, vol. 8, art. no. 01066. doi: https://doi.org/10.1051/e3sconf/20160801066.

4. Milykh V.I., Shilkova, L. V. Characteristics of a cylindrical inductor of a rotating magnetic field for technological purposes when it is powered from the mains at a given voltage. *Electrical Engineering & Electromechanics*, 2020, no. 2, pp. 13-19. doi: https://doi.org/10.20998/2074-272X.2020.2.02.

5. Ibragimov R.A., Korolev E.V., Kayumov R.A., Deberdeev T.R., Leksin V.V., Sprince A. Efficiency of activation of mineral binders in vortex-layer devices. *Magazine of Civil Engineering*, 2018, vol. 82, no. 6, pp. 191-198. doi: https://doi.org/10.18720/MCE.82.17.

6. Wołosiewicz-Głąb M., Foszcz D., Saramak D., Gawenda T., Krawczykowski D. Analysis of a grinding efficiency in the electromagnetic mill for variable process and feed parameters. *E3S Web of Conferences*, 2017, vol. 18, art. no. 01012. doi: https://doi.org/10.1051/e3sconf/20171801012.

7. Całus D., Makarchuk O. Analysis of interaction of forces of working elements in electromagnetic mill. *Przegląd Elektrotechniczny*, 2019, vol. 95, no. 12, pp. 64-69. doi: https://doi.org/10.15199/48.2019.12.12.

8. Wołosiewicz-Głąb M., Pięta P., Foszcz D., Niedoba T., Gawenda T. Adjustment of limestone grinding in an electromagnetic mill for use in production of sorbents for flue gas desulphurization. *Physicochemical Problems of Mineral Processing*, 2019, vol. 55, no. 3, pp. 779-791. doi: https://doi.org/10.5277/ppmp19011.

9. Ogonowski S., Wołosiewicz-Głąb M., Ogonowski Z., Foszcz D., Pawełczyk M. Comparison of Wet and Dry Grinding in Electromagnetic Mill. *Minerals*, 2018, vol. 8, no. 4, art. no. 138. doi: https://doi.org/10.3390/min8040138.

10. Zhakirova N., Salakhov R., Sassykova L., Khamidullin R., Deberdeev T., Yalyshev U., Khamidi A., Seilkhanov T. Increasing the Yield of Light Distillates by Wave Action on Oil Raw Materials. *Eurasian Chemico-Technological Journal*, 2021, vol. 23, no. 2, pp. 125-132. doi: https://doi.org/10.18321/ectj1083.

11. Kovalev A.A., Kovalev D.A., Grigoriev V.S., Litti Y.V. The vortex layer apparatus as a source of low-grade heat in the process of pretreatment of the substrate before anaerobic digestion. *IOP Conference Series: Earth and Environmental Science*, 2021, vol. 938, no. 1, art. no. 012004. doi: https://doi.org/10.1088/1755-1315/938/1/012004.

12. *Mixing machine AVS-100. Electromagnetic mill*. Available at: https://globecore.com/products/magnetic-mill/mixing-machine-avs-100/ (Accessed 20.02.2022).

13. Ogonowski S., Ogonowski Z., Pawełczyk M. Multi-Objective and Multi-Rate Control of the Grinding and Classification Circuit with Electromagnetic Mill. *Applied Sciences*, 2018, vol. 8, no. 4, art. no. 506. doi: https://doi.org/10.3390/app8040506.

14. Krawczykowski D., Foszcz D., Ogonowski S., Gawenda T., Wołosiewicz-Głąb M. Analysis of the working chamber size influence on the effectiveness of grinding in electromagnetic mill. *IOP Conference Series: Materials Science and Engineering*, 2018, vol. 427, art. no. 012033. doi: https://doi.org/10.1088/1757-899X/427/1/012033.

15. Ogonowski S. On-Line Optimization of Energy Consumption in Electromagnetic Mill Installation. *Energies*, 2021, vol. 14, no. 9, art. no. 2380. doi: https://doi.org/10.3390/en14092380.

16. Styła S., Mańko M. A reluctance model of an electromagnetic mill using the stator of an asynchronous motor as an inductor. *Przegląd Elektrotechniczny*, 2020, vol. 96, no. 1, pp. 254-257. doi: https://doi.org/10.15199/48.2020.01.58.

17. Milykh V.I., Shilkova L.V. Numerical-experimental analysis of the magnetic field of a magnetic separator inductor on the basis of an asynchronous motor. *Bulletin of NTU «KhPI». Series: Electric machines and electromechanical energy conversion*, 2018, no. 5 (1281), pp. 104-109. (Ukr).

18. Makarchuk O., Calus D., Moroz V. Mathematical model to calculate the trajectories of electromagnetic mill operating elements. *Technical Electrodynamics*, 2021, no. 2, pp. 26-34. doi: https://doi.org/10.15407/techned2021.02.026.
19. Milykh V.I., Shilkova L.V. Control current method of the concentration of ferromagnetic elements in the working chamber of the technological inductor of magnetic field during its operation. *Electrical Engineering & Electromechanics*, 2020, no. 5, pp. 12-17. doi: https://doi.org/10.20998/2074-272X.2020.5.02.
20. Shcherban' E.M., Stel'makh S.A., Beskopylny A., Mailyan L.R., Meskhi B., Shuyskiy A. Improvement of Strength and Strain Characteristics of Lightweight Fiber Concrete by Electromagnetic Activation in a Vortex Layer Apparatus. *Applied Sciences*, 2021, vol. 12, no. 1, art. no. 104. doi: https://doi.org/10.3390/app12010104.
21. Krauze O., Buchczik D., Budzan S. Measurement-Based Modelling of Material Moisture and Particle Classification for Control of Copper Ore Dry Grinding Process. *Sensors*, 2021, vol. 21, no. 2, art. no. 667. doi: https://doi.org/10.3390/s21020667.
22. Styła S. Analysis of temperature distribution in electromagnetic mill. *Przegląd Elektrotechniczny*, 2016, vol. 92, no. 3, pp. 103-106. doi: https://doi.org/10.15199/48.2016.03.25.
23. Vlasov A.B., Mukhin E.A. Methodology for calculating the temperature of the windings of an electric machine based on quantitative thermography. *Vestnik of MSTU*, 2011, vol. 14, no. 4, pp. 671-680. (Rus).
24. Yang Y., Bilgin B., Kasprzak M., Nalakath S., Sadek H., Preindl M., Cotton J., Schofield N., Emadi A. Thermal management of electric machines. *IET Electrical Systems in Transportation*, 2017, vol. 7, no. 2, pp. 104-116. doi: https://doi.org/10.1049/iet-est.2015.0050.
25. Lundmark S.T., Acquaviva A., Bergqvist A. Coupled 3-D Thermal and Electromagnetic Modelling of a Liquid-cooled Transverse Flux Traction Motor. *2018 XIII International Conference on Electrical Machines (ICEM)*, 2018, pp. 2640-2646. doi: https://doi.org/10.1109/ICELMACH.2018.8506835.
26. Milykh V.I., Tymin M.G. A comparative analysis of the parameters of a rotating magnetic field inductor when using concentric and loop windings. *Electrical Engineering & Electromechanics*, 2021, no. 4, pp. 12-18. doi: https://doi.org/10.20998/2074-272X.2021.4.02.
27. Ostashevskiy N.A., Shayda V.P., Petrenko A.N. Research into thermal state of a frequency-controlled asynchronous motor by means of a finite element method. *Electrical Engineering & Electromechanics*, 2011, no. 5, pp. 39-42. (Rus).
28. Kazi S.N. (Ed.) *Heat Transfer Phenomena and Applications*. London, United Kingdom, IntechOpen, 2012. doi: https://doi.org/10.5772/3391.
29. Ostashevskiy N.A., Petrenko A.N., Yurieva O.Yu. *Teplovi rozrakhunky elektrychnykh mashyn* [Thermal calculations of electric machines]. Kharkiv, O.M. Beketov NUUEKh Publ., 2020. 450 p. (Ukr).
30. *The Engineering ToolBox*. Available at: https://www.engineeringtoolbox.com (Accessed 20.02.2022).
31. *Materials Thermal Properties Database*. Available at: https://thermtest.com/thermal-resources/materials-database (Accessed 20.02.2022).
32. Duong M.T., Chun Y.-D., Park B.-G, Kim D.-J, Choi J.-H, Han P.-W. Thermal analysis of a high speed induction motor considering harmonic loss distribution. *Journal of Electrical Engineering and Technology*, 2017, vol. 12. pp. 1503-1510. doi: https://doi.org/10.5370/JEET.2017.12.4.1503.
33. Shams Ghahfarokhi P., Podgornovs A., Kallaste A., Cardoso A.J.M., Belahcen A., Vaimann T., Asad B., Tiismus H. Determination of Heat Transfer Coefficient from Housing Surface of a Totally Enclosed Fan-Cooled Machine during Passive Cooling. *Machines*, 2021, vol. 9, no. 6, art. no. 120. doi: https://doi.org/10.3390/machines9060120.
34. *SMath Studio*. Available at: https://smath.com (Accessed 20.02.2022).

Received 11.08.2022
Accepted 25.10.2022
Published 06.05.2023

V.I. Milykh[1], *Doctor of Technical Science, Professor,*
V.P. Shaida[1], *PhD, Associate Professor,*
O.Yu. Yurieva[1], *PhD, Associate Professor,*
[1] National Technical University «Kharkiv Polytechnic Institute», 2, Kyrpychova Str., Kharkiv, 61002, Ukraine,
e-mail: mvikemkpi@gmail.com (Corresponding Author), vpsh1520@gmail.com; ele6780@gmail.com

How to cite this article:
Milykh V.I., Shaida V.P., Yurieva O.Yu. Analysis of the thermal state of the electromagnetic mill inductor with oil cooling in stationary operation modes. *Electrical Engineering & Electromechanics*, 2023, no. 3, pp. 12-20. doi: https://doi.org/10.20998/2074-272X.2023.3.02